

# Using Small-Angle Neutron Scattering to Study the Solution Conformation of *N*-(2-Hydroxypropyl)methacrylamide Copolymer–Doxorubicin Conjugates

Alison Paul,<sup>\*,†</sup> Maria J. Vicent,<sup>\*,‡,§</sup> and Ruth Duncan<sup>§</sup>

School of Chemistry, Cardiff University, Main Building, Park Place, Cardiff CF10 3AT, United Kingdom,  
Centro de Investigación Príncipe Felipe, Av. Autopista del Saler 16, E-46013 Valencia, Spain, and Welsh  
School of Pharmacy, Cardiff University, Redwood Building, King Edward VII Avenue, Cardiff CF10 3XF,  
United Kingdom

Received September 27, 2006; Revised Manuscript Received February 14, 2007

Our past research developed two *N*-(2-hydroxypropyl)methacrylamide (HPMA) copolymer–doxorubicin (Dox) conjugates that became the first synthetic polymer–anticancer conjugates to be evaluated clinically. The first, FCE28068, contained Dox bound to the polymeric carrier via a tetrapeptidic linker (glycine-phenylalanine-leucine-glycine (GFLG)) ( $M_w \sim 30\,000$  g/mol;  $\sim 8$  wt % drug), and the second, FCE28069, contained additionally galactosamine (Gal) ( $M_w \sim 30\,000$  g/mol;  $\sim 7.5$  wt % Dox) again bound by a GFLG linker. Galactosamine was included to promote hepatocyte/hepatoma targeting via the asialoglycoprotein receptor. Both conjugates showed antitumor activity and were clinically less toxic than free Dox (2–5 fold). However, despite their similar chemical characteristics, the conjugates displayed a significantly different maximum-tolerated dose (MTD) in patients. The aim of this study, therefore, was to use small-angle neutron scattering (SANS) to explore the solution behavior of a small library of HPMA polymer conjugates including FCE28068, FCE28069, and their pharmaceutical formulations, plus as reference compounds HPMA copolymer–GFLG conjugates containing aminopropanol (Ap) or galactosamine (Gal) alone (i.e., without Dox). The SANS data obtained showed that HPMA copolymer–GFLG–Ap conjugates (containing 5 and 10 mol % side chains) showed evidence of polymer aggregation, however, no indication of aggregation was observed for FCE28068 and FCE28069 over the concentration range studied (2.5–50 mg/mL). Clear differences in the scattering behavior for the two conjugates were observed at equivalent concentration. Data were best fitted by a model for polydisperse Gaussian coils, and the HPMA copolymer–Dox conjugate with Gal (FCE28069) exhibited a larger radius of gyration ( $R_g$ ) (by  $\sim 2.5$  nm) compared to FCE28068. In conclusion, we have shown that SANS will be a valuable tool to elucidate conformation–performance relationships for polymer–drug conjugates.

## Introduction

Following the suggestion that polymer–drug conjugates might be useful for drug targeting,<sup>1</sup> systematic optimization of conjugate structure led us to design FCE28068 (PK1) and FCE28069 (PK2), both *N*-(2-hydroxypropyl)methacrylamide (HPMA) copolymer–doxorubicin (Dox) conjugates (reviewed in ref 2) that became the first synthetic polymer-based anticancer drug conjugates to be tested in man.<sup>3</sup> Since then, more than 10 anticancer drug conjugates have followed into clinical development (reviewed in ref 4). Currently, a polyglutamic acid–paclitaxel conjugate (XYOTAX) is showing particular promise for the treatment of women with nonsmall cell lung cancer.<sup>5</sup> Polymer–drug conjugates are complex macromolecules having a tripartite structure as a minimum comprising the polymer backbone, a biodegradable polymer–drug linker, and a bioactive antitumor agent. In some cases, targeting residues and imaging moieties are also added. The biological rationale for design of polymer conjugates, their mechanism of action, clinical status,

and the challenges for preclinical and clinical use have all recently been reviewed.<sup>4–6</sup> The FCE28068 conjugate tested clinically was synthesized by Dox aminolysis of an HPMA copolymer precursor containing  $\sim 5$  mol % methacryloyl(MA)-G(D,L)FLG-*p*-nitrophenoxo (ONp) side chains to give a conjugate of  $M_w \sim 30\,000$  g/mol and a Dox content of  $\sim 8$  wt % (free Dox  $< 2$  % total). In Phase I clinical trials,<sup>3</sup> the PK1 pharmaceutical formulation<sup>7</sup> was administered by short intravenous (i.v.) infusion every three weeks to patients with chemotherapy resistant cancer. Aware of the potential osmotic impact of a macromolecular prodrug, the infusion rate (4.16 mL/min) and concentration (2 mg/mL Dox-equiv) were kept the same during dose escalation and infusion time was gradually extended. The maximum-tolerated dose (MTD) (the MTD is the dose above which the side effects are too serious to go higher) of PK1 was 320 mg/m<sup>2</sup> (Dox-equiv). This dose is 4–5 fold higher than the usual free Dox dose used clinically. The dose-limiting toxicity seen for FCE28068 was typical of anthracyclines (neutropenia and mucositis), and activity was also observed in chemotherapy resistant patients. Subsequently, FCE28069 (an HPMA copolymer–GFLG–Dox conjugate containing galactosamine) was also evaluated clinically.<sup>8</sup> Designed to promote multivalent targeting via the hepatocyte asialoglycoprotein receptor to improve treatment of primary liver cancer,<sup>2</sup> this conjugate was the first synthetic biomimetic (of an asialoglycoprotein) conjugate. In this case, the HPMA

\* Authors to whom correspondence should be addressed. (A. P.): Phone: +44(0)2920 870419. Fax: +44(0)2920 874030. E-mail: paula3@cardiff.ac.uk. (M.J.V.): Phone: +34 963289681 (ext. 1303#). Fax: +34 963289701. E-mail: mjvicent@cipf.es.

<sup>†</sup> School of Chemistry, Cardiff University.

<sup>‡</sup> Centro de Investigación Príncipe Felipe.

<sup>§</sup> Welsh School of Pharmacy, Cardiff University.

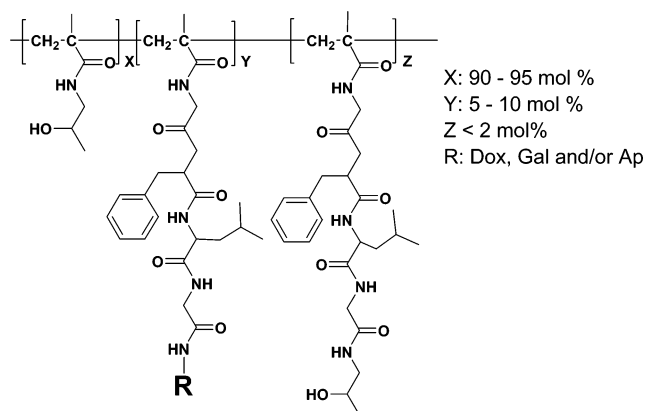


**Figure 1.** Conjugate structures.

copolymer precursor was synthesized using a monomer feed ratio of HPMA:MA-peptide-ONp adjusted to 90:10 to provide the additional pendent side chains needed to load both Dox and galactosamine. FCE28069 has a slightly lower molecular weight ( $M_w \sim 25\,000$  g/mol), because of the polymerization kinetics, a Dox content of  $\sim 7.5$  wt %, and galactosamine content of 1.5–2.5 mol %. Although the dose-limiting toxicities seen for FCE28069 were typical of anthracyclines and were similar to those seen for FCE28068, its MTD was significantly lower ( $160$  mg/m<sup>2</sup> Dox-equiv).<sup>8</sup> Several primary liver cancer patients displayed a partial response or stable disease. It is not clear why FCE28068 and FCE28069 have such different MTDs. FCE28069 is less water-soluble because of the higher loading of hydrophobic (FL) peptidyl side chains. Although this may explain why infusion using the same conditions employed for FCE28068 caused pain which led to a reduction in the infusion rate (2 mL/min) and a diluted infusion solution (1.0 mg/mL Dox-equiv),<sup>8</sup> it is puzzling why the overall pattern of dose-limiting toxicity did not change.

Recent experiments using small-angle neutron scattering (SANS) allowed us to study pH-dependent changes in conformation of endosomolytic polyamidoamines<sup>9</sup> and also to define the radius of gyration ( $R_g$ ) of HPMA copolymer conjugates containing both Dox and the aromatase inhibitor aminogluthimide (AGM)<sup>10</sup> as a combination therapy. Therefore, the aim of this study was to use SANS to see if it was possible to identify subtle changes in the coil structure of FCE28068 and FCE28069, and a library of compounds was used to elaborate detailed structure–property relationships (summarized in Figure 1 and Table 1).

Aminolyzed (with 1-aminopropan-2-ol (Ap)) HPMA copolymer intermediates bearing both 5 and 10 mol % side chains and HPMA copolymer–GFLG–galactosamine (Gal) (10 mol % side chains) were first synthesized as reference materials. SANS has been widely used to investigate polymer conformation in solution, for example, polyelectrolytes,<sup>11,12</sup> polymer–surfactant interactions,<sup>13</sup> and recently dendrimer conformation.<sup>14,15</sup> To the best of our knowledge, however, outside of our previous preliminary study,<sup>10</sup> SANS has not previously been used to evaluate the solution properties of polymer–drug conjugates, so it was first necessary to establish the baseline conditions for experimentation. Using relatively high sample concentrations sometimes required for good SANS data can promote polymer–polymer interactions, affecting the scattering observed and introducing an additional structure factor that will lead to artifacts. Thus, initial studies were undertaken to establish the minimum concentration that could be used to detect scattering while at the same time attempting to mimic the concentration used during patient administration (50 mg/mL for

FCE28068).<sup>7</sup> The range of concentrations chosen ranged from the relatively low conjugate concentrations that might be expected in blood following dilution to the higher concentrations that might be anticipated in lysosomes following endocytic internalization. To mimic the pH of lysosomes, experiments were also undertaken in D<sub>2</sub>O at pH 5.5 with additional NaCl (0.1 M) to mimic physiological ionic strength. Finally, it was necessary to establish the most appropriate mathematical model to fit the data, to define conjugate shape, and to allow estimation of the radius of gyration ( $R_g$ ).

## Materials and Methods

**Materials.** HPMA copolymer precursors carrying GFLG–ONp side chains (either 5 or 10 mol %;  $M_w \sim 20\,000$ – $25\,000$  g/mol and  $M_w/M_n = 1.3$ – $1.5$ ) were from Polymer Laboratories Ltd, U.K. The ONp content was calculated using  $\epsilon_{274\text{ nm}} = 9500$  L/mol/cm (in DMSO). Anhydrous dimethyl formamide (DMF) and dimethyl sulfoxide (DMSO) were from Sigma-Aldrich, U.K., HPLC grade solvents were from Fisher Scientific, U.K., and D<sub>2</sub>O was from Goss Scientific, U.K. All other reagents were of general laboratory grade and were from Aldrich unless otherwise stated. FCE28068 and FCE28069 were kindly supplied by Pharmacia, Italy (Table 1). The FCE28068 and FCE28069 formulation samples were prepared as described below.

**Methods.** *Synthesis of the HPMA Copolymer–Aminopropanol Conjugates.* HPMA copolymer precursor containing either 5 or 10 mol % side chains (1 equiv in relation to ONp) was dissolved in a minimal volume of dry DMSO. Then, Ap (3 equiv) was added dropwise, and the release of ONp was monitored spectrophotometrically at 400 nm. The reaction was left for 3 h at room temperature (RT). Then, the solvent was partly removed under high vacuum, and the residue was precipitated into a vigorously stirred mixture of acetone:Et<sub>2</sub>O (4:1). It was filtered off and washed with acetone and diethyl ether, and the conjugate was then dissolved in a minimal amount of water, was purified by dialysis against H<sub>2</sub>O ( $M_w$  cutoff 2000 g/mol), and was freeze-dried. The overall yield based on polymer weight was 80–90%.

*HPMA Copolymer–Galactosamine Conjugate.* An HPMA copolymer precursor containing 10 mol % side chains was used, and 1 equiv (in relation to ONp groups) was dissolved in a minimal volume of dry DMSO. Galactosamine hydrochloride (0.25 equiv) was added in DMSO solution, and the pH was adjusted to 8 with triethylamine. The reaction was monitored by measuring ONp release at 400 nm and also by thin-layer chromatography (TLC) using 2-propanol:pyridine:AcOH:H<sub>2</sub>O (SiO<sub>2</sub>, 8:8:1:4 v/v) as the mobile phase. The  $R_f$  (distance travelled by component spot divided by distance travelled by solvent front) of galactosamine was 0.51, and HPMA copolymer galactosamine conjugate remains at the origin; the  $R_f$  of ONp was 0.9. Complete disappearance of galactosamine was determined by TLC after 3 h at RT. Then, an excess of Ap (1 equiv) was added and the solvent was partly removed under high vacuum. The product was then isolated and freeze-dried as described above. The overall yield based on polymer weight was  $\sim 85\%$ .

*Preparation of FCE28068 and FCE28069 Pharmaceutical Formulations.* All drugs are administered to patients as pharmaceutical formulations previously optimized to ensure stability during storage and, for intravenous administration, to ensure rapid dissolution and acceptable pH. The composition of the FCE28068 and FCE28069 formulations is given in Table 2, and they were prepared following the indications described in Cavallo et al.<sup>7</sup> Briefly, the active drug (FCE28068 or FCE28069, 8.5 mg Dox-equiv) together with a soluble filler (lactose), a cosolubilizer (polysorbate 80), and a very low concentration of an organic solvent (ethanol) were completely solubilized in water and were freeze-dried to obtain PK1/PK2 lyophilized formulations.

*SANS Evaluation of HPMA Copolymer Conjugates.* SANS experiments were performed using the LOQ time-of-flight diffractometer at ISIS (Rutherford Appleton Laboratories, Oxford) or using the D22

**Table 1.** Characteristics of the Conjugates

compound	side chain content (mol %)	Dox <sup>f</sup> content (wt %)	Gal content (mol %)	Dox release (% at 24 h)	MTD (mg/m <sup>-2</sup> Dox-equiv)	R <sub>g</sub> <sup>d</sup> (nm ± 0.5)
Control Conjugates <sup>a</sup>						
HPMA copolymer–GFLG–Ap	5	n/a	n/a	n/a	n/a	ND
HPMA copolymer–GFLG–Ap	10	n/a	n/a	n/a	n/a	ND
HPMA copolymer–GFLG–Gal–Ap	10	n/a	≈2	n/a	n/a	4.5
Conjugates in Clinical Trials <sup>b</sup>						
HPMA copolymer–GFLG–Dox (FCE28068)	5	8.5	n/a	60 <sup>e</sup>	320	7.8
HPMA copolymer–GFLG–Gal–Dox (FCE28069)	10	7.5	1.5–2.5	60 <sup>e</sup>	160	10.5
Pharmaceutical Formulations <sup>a,c</sup>						
HPMA copolymer–GFLG–Dox (lyophilized FCE28068)	5	8.5	n/a	n/a	320	7.8
HPMA copolymer–GFLG–Gal–Dox (lyophilized FCE28069)	10	7.5	1.5–2.5	n/a	160	9.0

<sup>a</sup> Synthesized as described in Materials and Methods section. <sup>b</sup> Kindly supplied by Pharmacia, Italy. <sup>c</sup> From ref 7. <sup>d</sup> Calculated using eq 3 ( $1/I(Q) \approx N_A d^2 / (\Delta\rho)^2 c M (Q^2 R_g^2 / 3 + 1)$ ) and considering polydispersity = 1.3. <sup>e</sup> From ref 27. <sup>f</sup> Abbreviations: Aminopropanol, Ap; doxorubicin, Dox; galactosamine, Gal; maximum tolerated dose, MTD; n/a, not applicable; ND, not determined.

**Table 2.** Clinical Formulations of FCE28068 and FCE28069<sup>c</sup>

	PK1	PK2
conjugate	100.0 mg <sup>a</sup>	116.7 mg <sup>a</sup>
lactose	100.0 mg	100.0 mg
polysorbate 80	1.7 mg	1.7 mg
ethanol <sup>b</sup>	17.7 $\mu$ L	17.7 $\mu$ L
water <sup>b</sup>	2.5 mL	2.5 mL

<sup>a</sup> Equivalent to approximately 8.5 mg of Dox. <sup>b</sup> Removed during freeze-drying. <sup>c</sup> From ref 7.

camera at the Institute Laue-Langevin (ILL), (Grenoble). HPMA copolymer, FCE28068, and FCE28069 solutions were prepared in D<sub>2</sub>O (pH 5.5, 0.1 M NaCl) at concentration of (2.5–50 mg/mL) and were placed in 2-mm path length quartz cells, mounted in a sample changer thermostated at 37 °C (±0.2). Data were collected and corrected for the scattering and transmission of the solvent and cell and were placed on an absolute intensity scale with reference to a flat scatterer (ILL) or a well-characterized polymer blend (ISIS). Scattering data are expressed in terms of the scattering vector  $Q$  which is given by  $Q = 4\pi/\lambda \sin(\theta/2)$  in which  $n$  is the refractive index for neutrons ( $n \approx 1$ ),  $\lambda$  is the wavelength, and  $\theta$  is the scattering angle. The neutron wavelengths used were between 2 and 10 Å (LOQ) and 6 Å (D22) to span  $Q$ -ranges of approximately 0.01–0.6 on D22 and 0.008–0.3 Å<sup>-1</sup> on LOQ.

The scattering intensity  $I(Q)$  is described in terms of the relative contributions of the form factor  $P(Q)$  (which describes the size and shape of the scattering body), the structure factor  $S(Q)$  (which describes interactions between different scattering bodies), and  $B_{inc}$  which is a flat background arising from incoherent scattering, principally from hydrogenated material within the sample.

$$I(Q) = \phi V_p (\Delta\rho)^2 P(Q) S(Q) + B_{inc} \quad (1)$$

$\phi V_p (\Delta\rho)^2$  is a sample-dependent scale factor dependent on the polymer volume fraction  $\phi$ , the volume of a single particle  $V_p$ , and contrast term  $(\Delta\rho)^2$  which describes the difference in scattering length density between the solvent and the polymer,  $\Delta\rho = \rho_{solvent} - \rho_{polymer}$  ( $\rho_{solvent} = 6.4 \times 10^{10} \text{ cm}^{-2}$ ,  $\rho_{polymer} = 0.9 \times 10^{10} \text{ cm}^{-2}$ ). Since hydrogen and deuterium are at opposite ends of the scattering length density scale, in these systems contrast is achieved by dissolving the HPMA copolymer conjugates in D<sub>2</sub>O.

Scattering functions for simple geometric shapes are known.<sup>16</sup> To identify the adopted solution conformation, attempts were made to fit

the data to models for monodisperse spheres, polydisperse spheres, rigid and flexible rods, and polydisperse Gaussian coils.

First experiments examined the scattering behavior of serial dilutions of FCE28069 (starting at 50 mg/mL (5 wt %) to 2.5 mg/mL (0.25 wt %)) to investigate concentration-dependent aggregation effects or any influence of conjugate concentration on the conformation adopted in solution.

## Results

The polymer conjugates used and their characteristics are shown in Figure 1 and Table 2. The SANS scattering data obtained for FCE28069 during serial dilution from 50 mg/mL are shown in Figure 2. As conjugate concentration decreases, there is an accompanying decrease in scattering intensity consistent with the change in concentration ( $I(Q) \propto \phi$ ). No significant changes were seen in the overall shape of the scattering profile indicating that there are no major changes in conjugate conformation (e.g., change of aggregation state or sphere–rod transition). Normalization of the data to remove the concentration contribution (the scattering data were divided by the solution volume fraction after subtraction of the incoherent background scattering) produced data sets that fall on a common curve (Figure 2 inset). This confirmed that there was no concentration-induced interaction between the polymer conjugate chains over the concentration range used (i.e., absence of a structure factor  $S(Q)$ ). Dilution experiments were also undertaken with FCE28068, and again no polymer interaction was seen, with the normalized data falling onto a common curve. Therefore, for all further comparative experiments, a polymer concentration of 50 mg/mL was used.

In the absence of a structure factor  $S(Q)$ , eq 1 may be rewritten as

$$\frac{I(Q) - B_{inc}}{\phi} \propto V_p (\Delta\rho)^2 P(Q) \quad (2)$$

Hence, the scattering data obtained for FCE28068 and FCE28069 (50 mg/mL) were plotted in the reduced form given by eq 2, which removed the background incoherent scattering plus the concentration and scattering length density dependence of the scattering. This gave a direct comparison of the form factor for

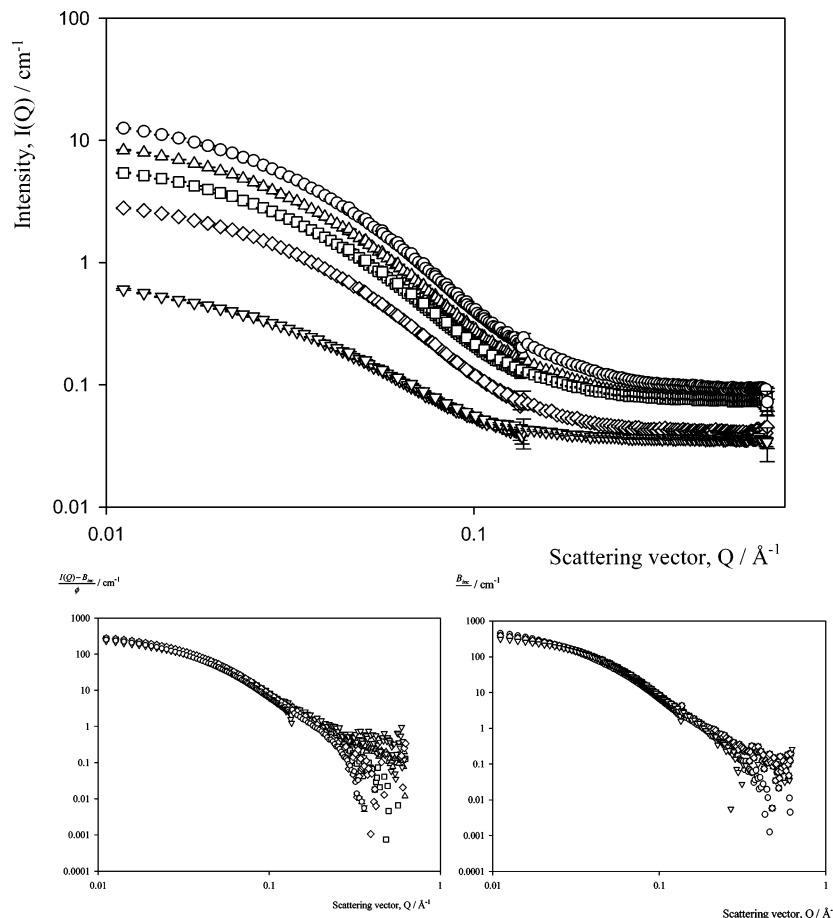


**Figure 2.** Effect of concentration on SANS scattering of FCE28069 in D<sub>2</sub>O. Key: 50 mg/mL (circles), 30 mg/mL (triangles), 10 mg/mL (squares), 5 mg/mL (diamonds), 2.5 mg/mL (inverted triangles). Bottom panel shows data normalized for concentration after subtraction of the incoherent background scattering [ $I(Q) - B_{\text{inc}}/\phi$  vs  $Q$ ] for FCE28068 (left) and FCE28069 (right).

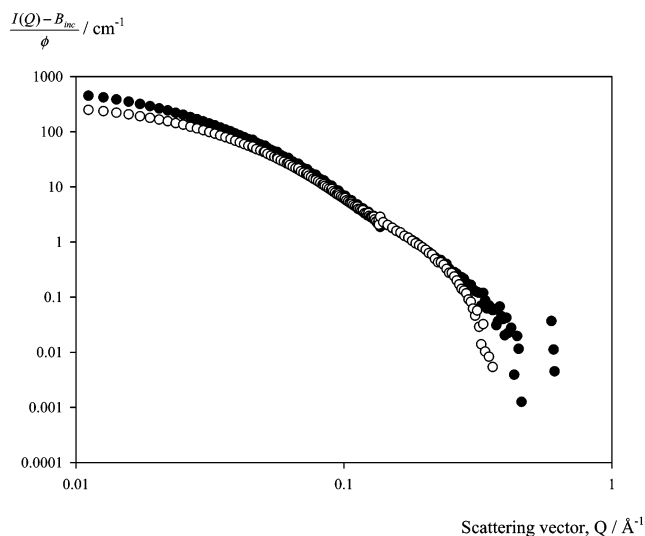


**Figure 3.** Comparison of normalized scattering data obtained for polymer conjugates (50 mg/mL) in D<sub>2</sub>O. Data were normalized by subtraction of the incoherent background scattering and division by sample volume fraction, as described in the text. Key: FCE28068 (open circles) and FCE28069 (closed circles).

each sample (Figure 3). On a log-log representation, the  $Q$  dependence (slope) of the scattering curves are indicative of the shape of the scattering body, and it can be seen that the form of the scattering profile is similar for both conjugates, indicating that their overall shape is similar.

Using a Zimm plot, values for the radii of gyration,  $R_g$ , could be estimated from a plot of  $1/(I(Q))$  versus  $Q^2$  using eq 3, where

$d$  is the bulk density and  $M$  is the molecular weight. This is valid at low  $Q$  values in dilute solution, in the limit  $QR_g < 1$ . The approach gave  $R_g$  values of  $9.3 \pm 0.5$  nm and  $11.3 \pm 0.5$  nm for FCE28068 and FCE28069, respectively (Figure 4a).

$$\frac{1}{I(Q)} \approx \frac{N_A d^2}{(\Delta\rho)^2 c M} \left( \frac{Q^2 R_g^2}{3} + 1 \right) \quad (3)$$

Attempts were made to fit the scattering data to a variety of theoretical form factors. It was clear that the monodisperse and polydisperse sphere models and the rigid and flexible rod models gave poor fits (Figure 4b) and physically unreasonable parameters. The best fit was obtained for a polydisperse Gaussian coil model, the form factor for which is given by eq 4, where  $R_g$  is the  $z$ -average of the radius of gyration. From this model, it is possible to obtain the  $R_g$  of the conjugates.

$$P(Q) = 2 \times \frac{\left( 1 + (p-1) \frac{(QR_g)^2}{1+2(p-1)} \right)^{(-1/(p-1))} + \left( \frac{(QR_g)^2}{1+2(p-1)} - 1 \right)}{(1 + (p-1) \left( \frac{(QR_g)^2}{1+2(p-1)} \right)^2)} \quad (4)$$

The absolute value for the  $R_g$  obtained is sensitive to the polydispersity,  $p$ . In this case, a  $p$  value of 1.3 was used as this reflects the polydispersity of the parent polymer. In addition, tests fits were carried out using a range of  $p$  values (1.0–2.0). Although the absolute  $R_g$  values for FCE28068 and FCE28069 changed from 7.2 to 8.9 ( $\pm 0.5$ ) nm and from 9.4 to 12.1 ( $\pm 0.5$ ) nm, respectively, the relative values were unaltered, with the



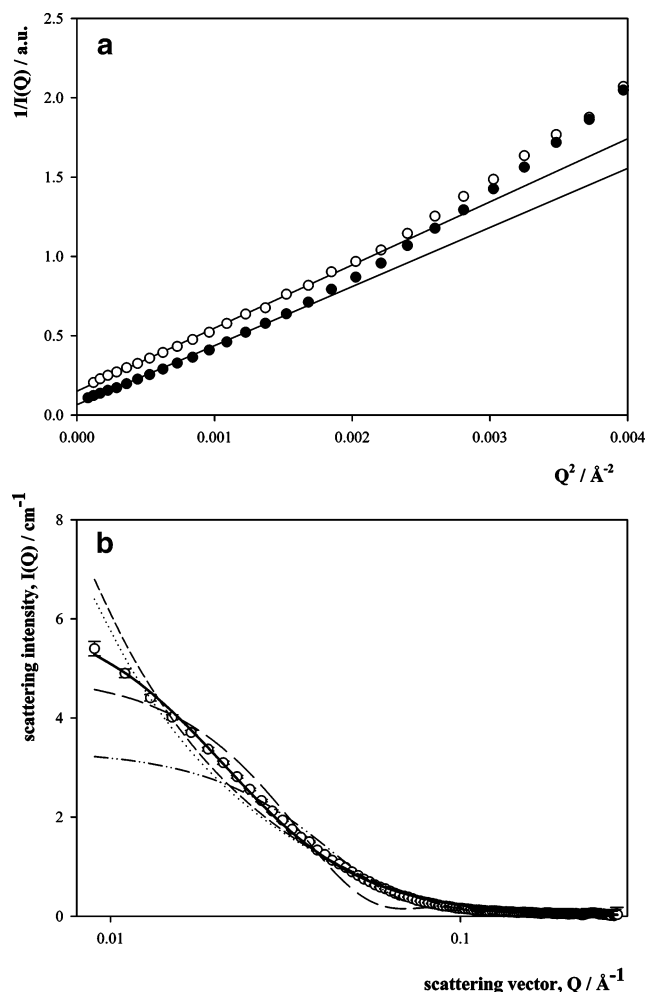


**Figure 4.** Expression of scattering data as Zimm plots and evaluation of the models with best fit. Panel (a) shows the Zimm plots for FCE28068 (open circles) and FCE28069 (closed circles) and the lines are best fits to low  $Q$  data made as described in text. Panel (b) shows the fits to the FCE28068 data obtained for various models. Key: Monodisperse spheres (long dash); polydisperse spheres (dash dot); rigid rods (short dash); flexible rods (dotted); polydisperse Gaussian coil (solid).

$R_g$  of FCE28069 consistently larger by  $\sim 2.5$  nm. Data for the conjugates FCE28068 and FCE28069 as pharmaceutical formulations were also fitted to this model. The radius of gyration for FCE28068 was identical to that in  $D_2O$  (pH 5.5, 0.1 M NaCl) ( $7.8 \pm 0.5$  nm). For FCE28069, a larger  $R_g$  ( $9.0 \pm 0.5$  nm) compared to FCE28068 was again obtained indicating a more open solution conformation.

Several control studies were undertaken to investigate the effect of the small changes in HPMA copolymer conjugate composition on scattering (Figure 5). Data were obtained for HPMA copolymer–GFLG–Ap (5 mol % side chains), HPMA copolymer–GFLG–Ap (10 mol % side chains), and HPMA copolymer–GFLG–Gal–Ap (10 mol % side chains). The scattering data obtained suggested aggregation (the upturn in scattering intensity at low  $Q$  values) of the HPMA copolymer–GFLG–Ap conjugates. This upturn is more pronounced for the polymer with 5% side chains, indicating that there is more aggregation for the 5% than 10% modification. This upturn was evident at all concentrations between 50 mg/mL and 5 mg/mL suggesting that aggregation was not disrupted by dilution. This prevented data fitting as it is not possible to separate contributions to the scattering from the  $S(Q)$  and  $P(Q)$  elements, according to eq 1. Once above the limit  $QR_g < 1$ , the scattering

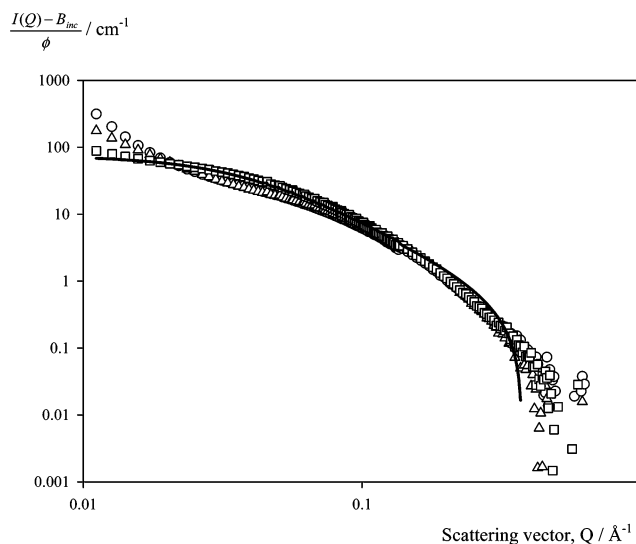


**Figure 5.** SANS scattering data obtained for the reference control polymers. Key: HPMA copolymer–GFLG–Ap (5 mol % side chains) (circles); HPMA copolymer–GFLG–Ap (10 mol % side chains) (triangles); HPMA copolymer–GFLG–Gal–Ap (10 mol % side chains) (squares). The line shown is the best fit and represents the polydisperse Gaussian coil model.

is no longer sensitive to the overall  $R_g$  of the polymer coil. As the scattering profiles obtained for the HPMA copolymer–GFLG–Ap 5 mol % and 10 mol % side chain conjugates were extremely similar, and in fact identical over the intermediate  $Q$  range, this would suggest no significant difference in the size of these conjugates.

There was a significant change in the scattering profile following conjugation of the Gal targeting group, and for the HPMA copolymer–GFLG–Gal–Ap conjugate, only the first few points of the scattering data show an upturn. So, for this data set, a reasonable estimate of  $R_g$  was obtained by fitting the polydisperse Gaussian coil model but excluding the first four points in the calculation. This gave an  $R_g$  estimate of  $4.5 \pm 0.5$  nm. ( $QR_g \sim 0.8$ ).

## Discussion

A growing number of studies have examined the physicochemical properties of nonviral vectors designed for gene delivery,<sup>17,18</sup> but the solution and physicochemical properties of polymer–drug conjugates have rarely been studied,<sup>19–24</sup> and the behavior of conjugates in physiologically relevant solutions is still poorly understood. Preclinical, physicochemical characterization of HPMA copolymer conjugates (including FCE28068, FCE28069, and HPMA copolymer–paclitaxel PNU166945) reported by Mendichi et al.<sup>23,24</sup> focused primarily on the determination of conjugate molecular weight distribution using size-exclusion chromatography coupled with viscosity and multiangle light scattering (MALS) fraction detection. These measurements were carried out in the organic elution solvents methanol and dimethyl formamide (DMF) containing LiBr (0.01 M) and  $CH_3COOH$  (0.05 M). Ulbrich et al. have used light-scattering techniques to study the solution properties of HPMA copolymers with *p*-nitroaniline as a model drug substance with various peptidyl linkers (these experiments were carried out in TRIS buffer).<sup>20</sup>

Drug conjugation can dramatically increase its solubility; for example, Dox conjugation increases solubility  $> 10$ -fold. Despite this high solubility, the dissolution rate of FCE28068 and FCE28069 in aqueous solution is relatively slow ( $> 30$  min).

To create faster dissolving, filter-sterilized, freeze-dried formulations suitable for i.v. administration during clinical use, addition of polysorbate 80 (as a dissolution enhancer), lactose, and a small amount of ethanol<sup>7</sup> was used for formulations that are stable during storage and that can be reconstituted with water for injection with a rapid dissolution time, <2 min.

It has become apparent that attachment of hydrophobic drugs to the hydrophilic HPMA copolymer platform can lead to the formation of unimolecular micelles, an effect that has been confirmed using HPMA copolymer–amino–ellipticine (APE) conjugates by measuring pyrene entrapment.<sup>25</sup> However, as pyrene entrapment is an indirect measurement that reports only on the local environment of the probe molecule itself, it is not possible to use this as conclusive evidence for a tightly coiled core–shell micellar structure. The propensity of HPMA copolymer–drug conjugates containing hydrophobic side chains ( $\pm$ drugs) to form unimolecular micelles or multimolecular aggregates in aqueous solution will influence conjugate biodistribution, potentially toxicity, and ultimately antitumor activity. The latter can be governed by accessibility of the intracellular activating enzymes to a peptidyl polymer–drug linker. It has been shown that increasing drug loading of Dox and APE decreases their rate of liberation by lysosomal thiol-dependent proteases.<sup>25,26</sup> The desire to gain physical evidence to support the assumed solution behavior of such conjugates led to the studies described here.

HPMA copolymer conjugate conformation in aqueous solution may be influenced by a combination of molecular weight of the polymer chain, drug loading, the pendent side chain content (including its statistical distribution along the main chain), as well as the presence of more hydrophilic targeting residues like Gal. It might be expected that addition of Gal would improve water solubility, but FCE28069 is less soluble than FCE28068 because of the increased content of relatively hydrophobic F-L-containing side chains. Although there was no discernible difference in the size and shape (a polydisperse Gaussian coil) of the HPMA copolymer–GFLG–Ap conjugates (5 and 10 mol %), the scattering data for these compounds showed an upturn at low  $Q$  values (Figure 5). Two factors might explain this scattering pattern: the existence of a small number of high molecular weight polymer chains would result in a rise in scattering at low  $Q$  values because of their large size ( $Q \propto 1/\text{size}$ ), and alternatively, the presence of intermolecular interaction/aggregation. Although it is currently not possible to distinguish between these two possibilities, similar aggregation effects were seen by Ulbrich et al. for HPMA copolymers with different Ap terminated peptidyl linkers at similar degrees of chain loading.<sup>20</sup> It is clear from our study that incorporation of Gal causes a significant change in the scattering and disrupts the intermolecular interaction/aggregation seen when using conjugates that contain side chains terminating in Ap alone. This effect is increased by the presence of Dox, where no intermolecular aggregation is indicated by the scattering profiles (Figure 2). To completely resolve these effects, further experiments are needed using less polydisperse conjugates and ideally selective deuteration of the conjugate components to highlight different parts of the structure (e.g., separate scattering contributions from the backbone and the linkers/drug molecules). In particular, a less broad molecular weight distribution will significantly enhance the detail and precision of information that can be extracted from the SANS data, in particular allowing further information on the shape as well as overall dimension of the conjugate in solution to be obtained.

Comparison of the scattering data obtained for FCE28068 and HPMA copolymer–GFLG (5 mol %)-Ap showed that Dox conjugation (equivalent to approximately 4–6 Dox molecules per chain) had a significant effect on solution conformation. No evidence of aggregation/interaction for the Dox-containing conjugate was seen. Significant differences were also apparent when comparing Dox-containing conjugates with and without Gal. Although FCE28068 and FCE28069 contain a similar amount of drug, the conjugate containing Gal had a larger  $R_g$  (Table 2). This may be attributable to the presence of the addition peptidyl side chains (unlikely because of the lack of difference between HPMA copolymer–GFLF–Ap containing 5 and 10 mol % side chains) or a reduction in the hydrophobic interactions between adjacent Dox molecules ( $\pi$ – $\pi$  stacking) because of the adjacent hydrophilic Gal residues. Clearly, overall conjugate conformation is a complex balance between the tendency of the polymer to form a compact coil structure, the side chains to cause intermolecular aggregation, and the hydrophobic/hydrophilic balance of substituted components that influence the conformation.

The larger  $R_g$  seen for FCE28069 might explain its lower MTD during clinical trial. Its more “open” coil structure could lead to greater exposure of conjugated drug to the biological environment, which might in turn also accelerate the drug release rate. Although the amount of drug released from both conjugates was the same after 24 h ( $\sim$ 60%) when measured in vitro, these studies did not establish the kinetics of release (a single enzyme concentration was used).<sup>27</sup> This possibility certainly warrants further investigation and illustrates the possibility of combining SANS and enzymology preclinically with a view to designing conjugates with better drug release profiles.

## Conclusions

The first detailed SANS analysis of a family of structurally related polymer–drug conjugates has been presented. With small changes in conjugate chemistry, subtle differences in solution properties were seen. These included the aggregation of HPMA copolymer–GFLG–Ap conjugates and differences in  $R_g$  for FCE28068 and FCE28069, two conjugates that have entered clinical trial. These results show that SANS will be a valuable tool for determining the structure activity relationships of this important new class of polymer therapeutics.

**Acknowledgment.** A. P. was supported by an EPSRC Platform Grant, EP/CO13220/1. M. J. V. was supported by a Marie Curie Individual Fellowship, Contract N° HPMF-CT-2002-01555. We thank Dr. P. C. Griffiths for critical reading of the manuscript and CLRC for allocation of beam time and grants toward consumables and travel. Drs. R. K. Heenan (ISIS) and I. Grillo (ILL) are thanked for their assistance with SANS experiments.

## References and Notes

1. Ringsdorf, H. *J. Polym. Sci., Polym. Symp.* **1975**, *51*, 135–153.
2. Duncan, R.; Kopecek, J. *Adv. Polym. Sci.* **1984**, *57*, 51–101. Duncan, R. *Anti-Cancer Drugs* **1992**, *3*, 175–210. Duncan, R. N-(2-Hydroxypropyl)methacrylamide copolymer conjugates. In *Polymeric Drug Delivery Systems*; Kwon, G. S., Ed.; Marcel Dekker, Inc.: New York, 2005; pp 1–92.
3. Vasey, P.; Kaye, S. B.; Morrison, R.; Twelves, C.; Wilson, P.; Duncan, R.; Thomson, A. H.; Murray, L. S.; Hilditch, T. E.; Murray, T.; Burtles, S.; Fraier, D.; Frigerio, E.; Cassidy, J. *Clin. Cancer Res.* **1999**, *5*, 83–94.
4. Duncan, R. *Nat. Rev. Cancer* **2006**, *6*, 688–701. Vicent, M. J.; Duncan, R. *Trends Biotechnol.* **2006**, *24*, 39–47. *Polymer Therapeutics: Polymers as Drugs, Conjugates and Gene Delivery Systems*; Satchi-Fainaro, R., Duncan, R., Eds.; Advances in Polymer Science 192 and 193; Springer: London, 2006.

- (5) Singer, J. W.; Shaffer, S.; Baker, B.; Bernareggi, A.; Stromatt, S.; Nienstedt, D.; Besman, M. *Anti-Cancer Drugs* **2005**, *16*, 243–254.
- (6) Duncan, R. Polymer-Drug conjugates. In *Handbook of Anticancer Drug Development*; Budman, D., Calvert, H., Rowinsky, E., Eds.; Lippincott, Williams & Wilkins: Baltimore, MD, 2002.
- (7) Cavallo, R.; Adami, M.; Magrini, R.; Colombo, G. *Proceedings 1st World Meeting APGI/APV*, Budapest, Hungary, May 9–11, 1995; p 843.
- (8) Seymour, L. W.; Ferry, D. R.; Anderson, D.; Hesslewood, S.; Jylan, P. J.; Poyner, R.; Doran, J.; Young, A. M.; Burtles, S.; Kerr, D. J. *J. Clin. Oncol.* **2002**, *20*, 1668–1676.
- (9) Griffiths, P. C.; Paul, A.; Khayat, Z.; Duncan, R.; Wan, K-W.; King, S. M.; Grillo, I.; Schweins, R.; Ferruti, P.; Franchini, J. *Biomacromolecules* **2004**, *5*, 1422–1427. Wan, K-W.; Malgesini, B.; Verpilio, I.; Ferruti, P.; Griffiths, P. C.; Paul, A.; Duncan, R. *Biomacromolecules* **2004**, *5*, 1102–1109. Khayat, Z.; Griffiths, P. C.; Grillo, I.; Heenan, R. K.; King, S. M.; Duncan, R. *Int. J. Pharm.* **2006**, *317*, 175–186.
- (10) Vicent, M. J.; Greco, F.; Nicholson, R. I.; Paul, A.; Griffiths, P. C.; Duncan, R. *Angew. Chem., Int. Ed.* **2005**, *44*, 2–6.
- (11) Nakamura, K.; Shikata, T.; Takahashi, N.; Kanaya, T. *J. Am Chem. Soc.* **2005**, *127*, 4570–4571.
- (12) Nishida, K.; Kaji, K.; Kanaya, T.; Shibano, T. *Macromolecules* **2002**, *35*, 4084–4089.
- (13) Aswal, V. K. *Chem. Phys. Lett.* **2003**, *371*, 371–377.
- (14) Ramzi, A.; Scherrenberg, R.; Joosten, J.; Lemstra, P.; Mortensen, K. *J. Phys. Chem. B* **2000**, *35*, 827–833.
- (15) Hedden, R. C.; Bauer, B. J. *Macromolecules* **2003**, *36*, 1829–1835.
- (16) Higgins, J.; Benoit, L. In *Polymer and Neutron Scattering*; Lovesy, S. W., Mitchell, E. W. J., Eds.; Clarendon Press: Oxford, U.K., 1996.
- (17) Konak, C.; Mrkvickova, L.; Nazarova, O.; Ulbrich, K.; Seymour, L. W. *Supramol. Sci.* **1998**, *5*, 67–74.
- (18) Oupicky, D.; Konak, C.; Ulbrich, K. *J. Biomater. Sci., Polym. Ed.* **1999**, *10*, 573–590.
- (19) Bohdanecky, M.; Bazilova, H.; Kopecek, J. *Eur. Polym. J.* **1974**, *10*, 405–410.
- (20) Ulbrich, K.; Konak, C.; Tuzar, Z.; Kopecek, J. *Makromol. Chem.* **1987**, *188*, 1261–1272.
- (21) Mendichi, R.; Rizzo, V.; Gigli, M.; Giacometti Schieroni A. *J. Liq. Chromatogr. Relat. Technol.* **1996**, *19*, 1591–1605.
- (22) Shiah, J. G.; Konak, C.; Spikes, J. D.; Kopecek, J. *J. Phys. Chem.* **1997**, *101*, 6803–6809.
- (23) Mendichi, R.; Rizzo, V.; Gigli, M. *Bioconjugate Chem.* **2002**, *13*, 1253–1259.
- (24) Mendichi, R.; Rizzo, V.; Gigli, M.; Giacometti, Scieroni, A. *J. Appl. Polym. Sci.* **1998**, *70*, 3–8.
- (25) Searle, F.; Gac-Breton, S.; Keane, R.; Dimitrijevic, S.; Brocchini, S.; Duncan, R. *Bioconjugate Chem.* **2001**, *12*, 711–718. Keane, R.; Gac-Breton, S.; Searle, F.; Duncan, R. *J. Pharm. Pharmacol.* **2000**, *52* (Suppl.), 52.
- (26) Greco, F.; Vicent, M. J.; Gee, S.; Jones, A. T.; Gee, J.; Nicholson, R. I.; Duncan, R. *J. Controlled Release* **2006**, *117*, 29–39.
- (27) Subr, V.; Strohalm, J.; Ulbrich, K.; Duncan, R.; Hume, I. C. *J. Controlled Release* **1992**, *18*, 123–132.

BM060925S